RSGC
Royal St. George's College

The Young Researcher

2022 Volume 6 | Issue 1

Investigation on the Effect of Infill Orientation on the Flexural Properties in FDM Parts

Alexander Barry

Recommended Citation
Barry, A. (2022). Investigation on the effect of infill orientation on the flexural properties in FDM parts. *The Young Researcher*, 6(1), 94-105. http://www.theyoungresearcher.com/papers/barry.pdf

ISSN: 2560-9815 (Print) 2560-9823 (Online) Journal homepage: http://www.theyoungresearcher.com

Investigation on the Effect of Infill Orientation on the Flexural Properties in FDM Parts

Alexander Barry

Parts made with Fused Deposition Modeling (FDM) are anisotropic, meaning that their properties are dependent on their orientation and the direction of forces. This study aimed to investigate how the infill orientation in FDM parts influences their flexural properties. Samples were created with either a 0° or 45° infill orientation and evaluated using a 3-Point Bending test. Samples with a 0° infill orientation had a brittle failure mode, lower coefficient of variation, higher yield strength, and higher flexural modulus, while samples with a 45° infill orientation had a ductile failure mode and a higher maximum force value. Samples with a 45° infill orientation had a higher flexural strain at failure, but samples of both infill orientations had similar flexural strength. This suggests that while both orientations result in similar flexural strengths, the 0° infill orientation is largely superior to the 45° infill orientation in terms of flexural properties.

Keywords: Fused deposition modeling (FDM), anisotropy, infill orientation, flexural properties

Additive Manufacturing (AM) is rapidly taking over many manufacturing industries, such as aerospace and robotics, due to its ability to create complex objects in a timely and cost-efficient manner. There are multiple types of AM, the main ones being Fused Deposition Modeling (FDM), stereolithography, and selective laser sintering [1]. FDM, also known as 3D printing, involves placing melted filament down in a path that cools and hardens, building the part layer by layer. FDM is cost-effective and among the most widespread AM processes [1], [2]. The reason for this cost-effectiveness is FDM's three main infill parameters: pattern, density, and orientation [3]. The infill pattern is a preset layout that determines the internal design of the part [4], [5], [6], [7]. The infill density is the area of the internal section for an FDM part that will be filled [3]. The infill orientation controls the angle at which the pattern is printed [5]. Due to the lack of uniformity, FDM parts are anisotropic, meaning they vary in strength in different orientations [5]. Although anisotropy is a principal quality of FDM parts, there has been no clear conclusion on how changing the infill orientation affects the flexural properties created when printing the filament.

I. Literature Review

A. Effect of Printing Parameters

Previous studies have investigated various printing parameters' effects on FDM parts. Some parameters directly affect how the filament is deposited, such as printing speed and temperature [8]-[10]. Higher printing speeds increase dimensional inaccuracies and weld lines, and in turn decrease structural integrity and strength [8], [9]. Higher printing temperatures lead to fewer dimensional inaccuracies and improved strength, due to the filament fusing better when more melted [8]. Additionally, other parameters, such as layer thickness and air gaps, control the characteristics of the print. Increasing layer thickness and air gap size decreases the precision of the part, and air gaps can lead to structural weaknesses [5], [8], [11].

B. Effect of Infill Parameters

Similarly, the three primary infill parameters have a large effect on the part's mechanical properties. Studies have found that higher infill densities generally result in higher mechanical strength and increased brittleness, but also raise manufacturing costs with increased print times and total filament usage [3]-[5], [8], [12]-[16]. While the infill pattern attribute has a negligible impact on cost, many sources have affirmed that it has a significant impact on a part's mechanical properties [4], [6], [12], [13], [17]. Although Gonabadi et al. [12] concluded that the infill pattern has little effect on tensile strength or Young's modulus, numerous other studies have challenged that conclusion, generally finding that the hexagonal and grid patterns are stiffer and have higher tensile strengths while triangular patterns have higher Young's moduli [4], [13], [17], [18]. Also, provided that the 0° orientation aligns with the direction of applied force, the mechanical properties generally decrease the more the infill orientation deviates away from 0° [17], [19]. Many studies have called attention to this anisotropy in all parts manufactured with FDM [5], [12], [15], [17], [19], [20].

C. Anisotropy in FDM Parts

While FDM parts' anisotropic nature has been identified, there remains a need for additional research on anisotropy. Casavola et al. [19] had shown up to a 50% and 60% decrease in maximum stress and energy absorption capability, respectively, between a filament orientation aligned vs not aligned with the load direction. Those results reveal that the anisotropy heavily affects the properties of FDM parts, and not understanding those anisotropic behaviors can cause items made with this process to be unusable. Despite its significance, there is still an absence of comprehensive data about the effect of infill orientation on FDM parts.

D. Research Gap

The goal of this research study was to answer the question: How does changing the infill orientation affect the flexural properties in parts made with FDM? This study measured the flexural properties of FDM parts while only changing the infill orientation to further investigate the effect of orientation. Furthermore, it builds upon the more general knowledge of the anisotropy in FDM parts by providing specific insight into how orientation affects the various flexural properties of those parts.

II. Material and Methods

A. Research Approach and Methods

This study used the mixed methods approach to investigate the effect of infill orientation on the flexural properties in FDM parts. Quantitative data were utilized to determine the mechanical properties of the samples. Qualitative data were utilized to record observations and failure modes. The quantitative and qualitative data collected were able to reliably validate the conclusions made in the study at hand.

The experimental research method was used in this study to determine the effect that the infill orientation of FDM parts had on their flexural properties. This method was used to identify the changes to the flexural properties caused by modifying the infill orientation, which provided enough evidence to thoroughly answer the research question.

B. Subject Selection

This study used the Acrylonitrile Butadiene Styrene (ABS) polymer and the grid infill pattern. ABS was chosen because it is one of the most common materials used in FDM and was chosen for many similar studies including [9], [11], and [19]. The grid infill was chosen due to it being one of the most common infill patterns and having no significant structural abnormalities. Infill orientations of 0° and 45° were chosen due to this infill pattern having four axes of symmetry, meaning those orientations would result in the largest amount of variation. The width selection required more analysis since the impact of the outer border on the overall characteristics was unknown. The border consisted of solidly printed lines of filament in the vertical and horizontal directions, which could skew the results of the test if the border represented a large part of the overall strength of the samples. 3-Point Bending tests were conducted on samples with a length of 96 mm, a thickness of 3 mm, and widths of 12.5 mm, 25 mm, and 37.5 mm. Even though the border made up a slightly larger portion of the smaller samples, all three widths resulted in almost identical properties. As a result, the width was chosen based on how consistently it was able to be printed, and that was determined using the coefficient of variation, a measurement of the variation and discrepancy in a data set. The 25 mm width resulted in samples that had the least coefficient of variation between the trials and thus was chosen to be used in this study.

C. Validity

The number of external factors that affected the results were minimized, and five replicates were done for each orientation to ensure that outliers would not heavily impact the data. Due to ABS being a polymer that shares many characteristics with a multitude of other polymers, the overall results of this study could be applied to FDM parts made from those similar polymers as well. This study focused on the general trends between the flexural properties of samples in different orientations and less on the individual strength values themselves. This means that if a part has a similar structure and infill to the samples in this experiment, the results would provide some insight into its properties. The tools used in this study were a dial caliper and a micrometer, both of which determined the dimensions of the samples with an accuracy of 0.001 mm. An Instron Universal Testing machine with a 3-Point Bending fixture was used to gather data about the strength and displacement of each of the samples. The Instron machine was accurate to within 0.5% of the measured force.

D. Procedure

In this study, ten samples made from ABS with dimensions of 96 mm by 25 mm by 3 mm were printed through FDM in a Stratasys© uPrint© SE. The samples had 100% infill density and the grid infill pattern. Five samples had a 0° infill orientation and five had a 45° infill orientation. The border width was set to the smallest setting, 0.1 mm. **Figure 1** provides a diagram illustrating the samples' infill pattern and orientation. The ten samples were labeled and then measured with a dial caliper, micrometer, and scale to determine the actual dimensions and weight of each sample. A 3-Point Bending test, depicted in **Figure 2**, was performed with an Instron Universal Testing machine with a 100 N load cell according to the specifications in the standard provided by ASTM [21]. Following those specifications, the test used a support span of 72 mm, had a 2.54 mm/min loading velocity, and ran until the samples had passed their point of ultimate strength. The tests provided values for time and force at displacement intervals of 0.0254 mm. The failure mode, which is the way that each sample broke, was manually recorded.

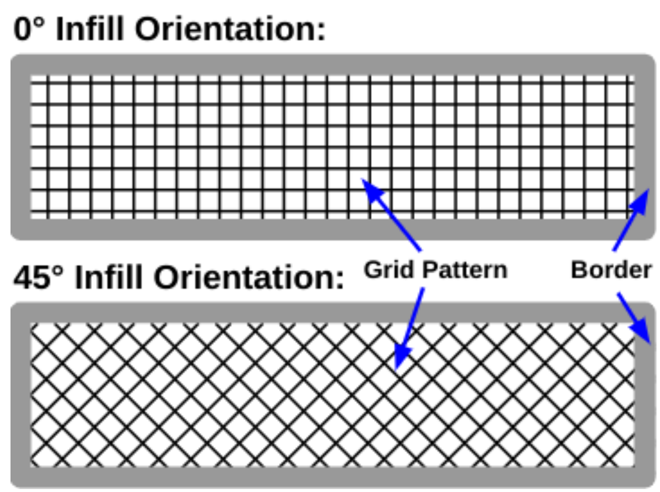

Figure 1. *Diagram of the samples detailing the grid infill pattern at 0° and 45° infill orientations. Note that the space in between the lines is only to emphasize the infill structure and no perceptible gaps were in the actual samples tested.*

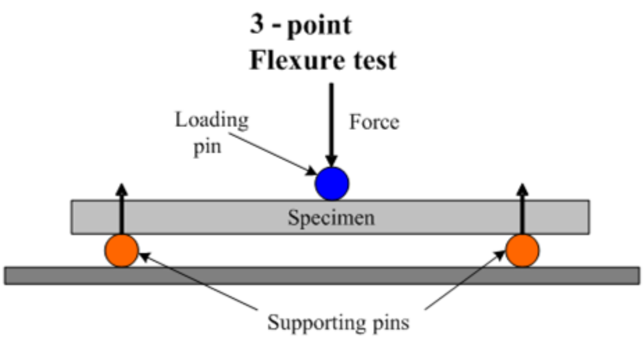

Figure 2. *Diagram of 3-Point Bending test used in this study. Adapted from [22]*

E. Data Analysis

The standard deviations, averages, and coefficients of variation were used to analyze the results of this study. The equations in the standard test method [21] were used to determine the flexural strength, flexural chord modulus of elasticity, and other related properties from the collected data. Graphs displaying force vs displacement and flexural stress vs flexural strain were created.

III. Results

A. General Characteristics

The basic dimensions and characteristics of the samples are displayed in **Table 1**. The graph of force vs displacement for all samples is displayed in **Figure 3**. The maximum force, displacement at the maximum force, and displacement at the point of failure for each sample are displayed in **Table 2**.

Sample No	Infill Orientation (degrees)	Length (cm)	Width (cm)	Thickness (cm)	Weight (g)	Density (g/cm^3)
1	0	9.589	2.494	0.320	6.441	0.841
2	0	9.602	2.506	0.318	6.441	0.842
3	0	9.589	2.497	0.321	6.441	0.839
4	0	9.611	2.499	0.315	6.441	0.851
5	0	9.608	2.497	0.321	6.441	0.836
6	45	9.601	2.501	0.325	6.532	0.836
7	45	9.595	2.492	0.317	6.532	0.862
8	45	9.605	2.498	0.319	6.486	0.848
9	45	9.590	2.496	0.321	6.532	0.850
10	45	9.580	2.499	0.332	6.532	0.822

Table 1. *The infill orientations, dimensions, weight, and density of tested samples.*

Sample No	Infill Orientation (degrees)	Max Force (N)	Displacement at Max Force (mm)	Displacement at Failure Point (mm)
1	0	89	9.1897	11.4732
2	0	92	8.8392	9.9263
3	0	90	9.6393	11.1430
4	0	94	8.5471	9.4615
5	0	90	9.3472	11.2979
6	45	91	11.8237	> 16
7	45	98	11.5138	> 16
8	45	98	11.5291	> 16
9	45	98	11.3614	> 16
10	45	91	12.1615	> 16

Table 2. *The maximum force exerted, the displacement at the point of maximum force, and the displacement at the point of failure for each sample during the 3-Point Bending tests.*

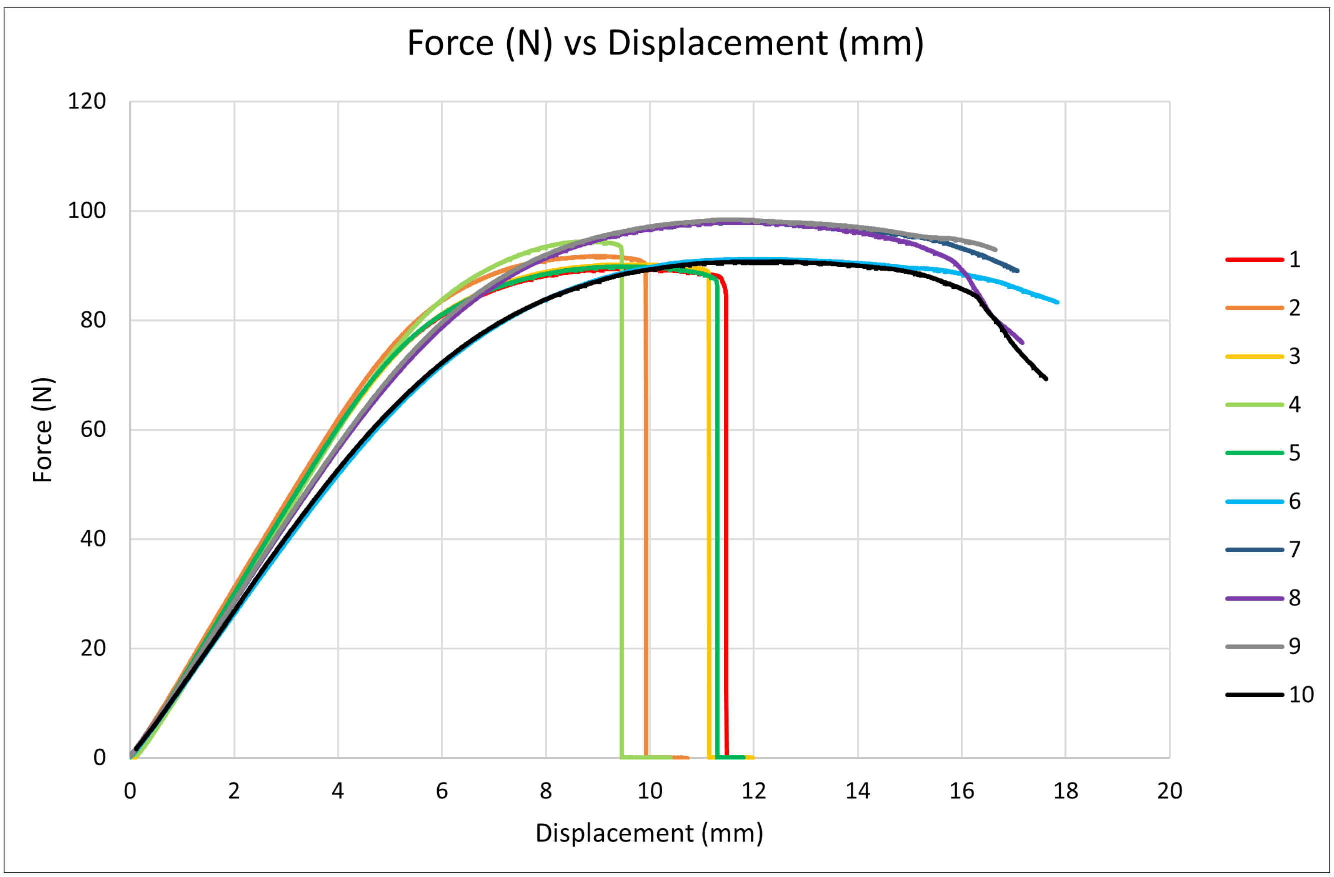

Figure 3. *Force vs displacement in a 3-Point Bending test, describing how much force was required to continuously push down the sample with the loading pin at a rate of 0.254 mm/min. Points were recorded in intervals of 0.05 mm or less of displacement.*

Samples 1 to 5, with a 0° infill orientation, exhibited a brittle failure mode, breaking cleanly into two pieces while or slightly after reaching its maximum loading force. In **Figure 3**, between a displacement of 9 mm and 12 mm, the value of force for samples 1 to 5 sharply dropped to 0 N. Alternatively, samples 6 to 10, with a 45° infill orientation, exhibited a ductile failure mode, deforming further instead of breaking after reaching its peak load. The values of force for samples 6 to 10 gradually decrease after the samples have reached their maximum load. **Figure 4** and **Figure 5** show pictures of samples 1 and 6, respectively, and visually display the difference in failure modes between the two samples.

All samples showed visual signs of plastic deformation visible as whitening at the central break location in the 0° samples and the middle of the 45° samples. However, plastic deformation was much more extensive in the 45° samples, as shown in **Figure 5**. The plastic deformation could be observed mainly on the tension side, where the material was being stretched apart. The plastic deformation across the center of the span affected both the material composing the border and the infill of the sample. The most deformation could be seen at the center of the samples.

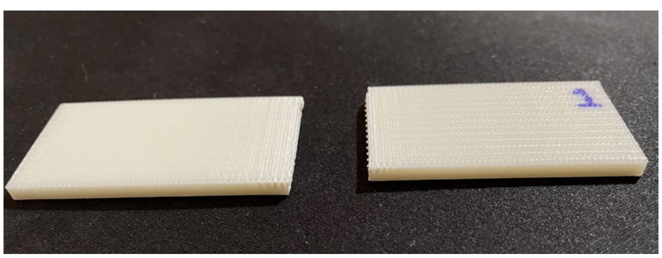

Figure 4. *Sample 1 (0° orientation) after it underwent its 3-Point Bending test and a brittle failure mode.*

Figure 5. *Sample 6 (45° orientation) after it underwent its 3-Point Bending test and a ductile failure mode.*

B. Calculated Mechanical Properties

All the properties calculated for the samples were found using the equations found in the standard method [21]**.** The flexural stress was calculated using (1) and the flexural strain was calculated using (2).

$$\boldsymbol{\sigma} = \frac{\mathbf{5}\boldsymbol{PL}}{\mathbf{2}\boldsymbol{bh^2}} \qquad (1)$$

where σ is the stress at the outer surface at mid-span, *P* is the applied force, *L* is the support span, *b* is the width of the beam, and *h* is the thickness of the beam.

$$\varepsilon = \frac{6\delta h}{L^2} \qquad (2)$$

where **ε** is the maximum strain at the outer surface, δ is the mid-span deflection, *L* is the support span, and *h* is the thickness of the beam.

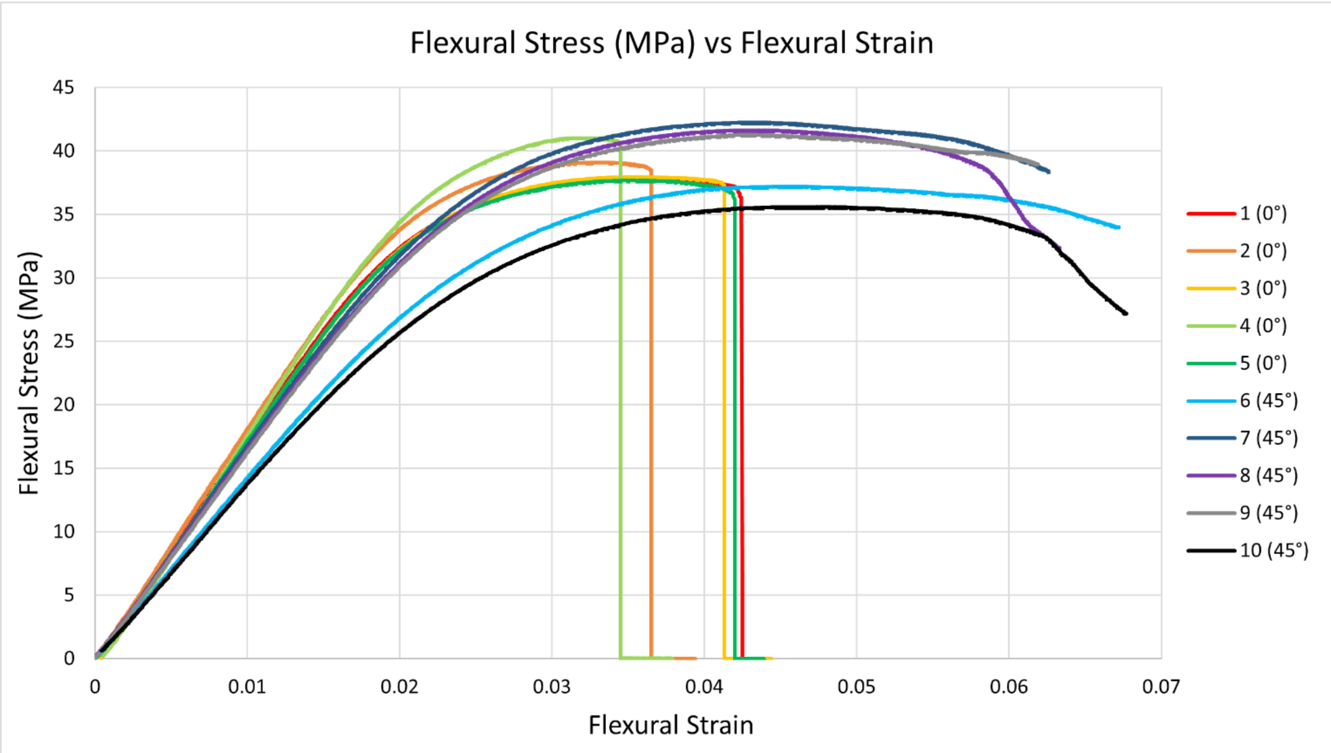

Figure 6. *Graph of flexural stress vs flexural strain during the 3-Point Bending test.*

Figure 6 shows the graph of flexural stress vs flexural strain. The 0° samples all followed a linear pattern, transitioned to a non-linear pattern until peaking around 39 MPa, and then suddenly decreased to 0 MPa. The 45° samples originally followed the same pattern as the 0° samples, starting linear and becoming non-linear, but did not experience any sudden drops, and instead more gradually decreased after peaking around 40 MPa.

The flexural strength, the flexural strain at the point of maximum flexural stress, the 0.2% offset yield stress, and the flexural chord modulus of elasticity for the samples are displayed in **Table 3**. The flexural chord modulus of elasticity was calculated according to (3).

$$E_f^{chord} = \frac{\Delta\sigma}{\Delta\varepsilon} \quad (3)$$

where E_f^{chord} is the flexural chord modulus of elasticity, $\Delta\sigma$ is the difference in flexural stress between the two selected strain points, and $\Delta\varepsilon$ is the difference between the two selected strain points.

The 0.2% offset line was calculated by finding the linear slope of the original data between the strain values of 0.1% and 0.3% and offsetting a line with that slope to the right by 0.2% flexural strain. The 0.2% offset yield stress was then found by determining the flexural stress value for the intersection point between the flexural stress vs flexural strain curve and the linear offset line. That 0.2% yield stress represents the amount of force required to cause permanent deformation of 0.2% in the sample. The mean, standard deviation, and coefficient of variation for each of the four properties displayed in **Table 3** are shown in **Table 4**.

Sample No	Infill Orientation (degrees)	Flexural Strength (MPa)	Flexural Strain at Max Flexural Stress	0.2% Offset Yield Stress (MPa)	Flexural Chord Modulus of Elasticity (MPa)
1	0	37.78	0.034	33.89	1,683
2	0	39.11	0.033	36.08	1,746
3	0	37.98	0.036	33.99	1,685
4	0	41.02	0.031	38.70	1,693
5	0	37.69	0.035	34.02	1,671
6	45	37.21	0.045	29.32	1,416
7	45	42.26	0.042	36.26	1,612
8	45	41.64	0.043	35.57	1,590
9	45	41.28	0.042	35.17	1,586
10	45	35.59	0.047	28.99	1,327

Table 3. *Flexural strength, flexural strain at the point of maximum flexural stress, the 0.2% offset yield stress, and the flexural chord modulus of elasticity are displayed for samples 1 to 5 during the 3-Point Bending tests.*

	Flexural Strength (MPa)		Flexural Strain at Maximum Flexural Stress		0.2% Offset Yield Stress (MPa)		Flexural Chord Modulus of Elasticity (MPa)	
Infill Orientation	Mean ± SD	CV	Mean ± SD	CV	Mean ± SD	CV	Mean ± SD	CV
0 degrees	38.72 ± 1.26	3.25%	0.0336 ± .0016	4.76%	35.34 ± 1.87	3.25%	1,695.56 ± 26.09	1.54
45 degrees	39.60 ± 2.68	6.76%	0.0436 ± .0018	4.04%	33.06 ± 3.21	6.76%	1,506.09 ± 114.15	7.58

Table 4. *The means, standard deviations, and coefficients of variation (CV) of the flexural strength, flexural strain at the point of maximum flexural stress, the 0.2% offset yield stress, and the flexural chord modulus of elasticity are displayed for each of the infill orientations evaluated.*

C. Summary of Research

Overall, samples 6 to 10 had higher maximum loads and higher flexural properties than samples 1 to 5, but lower flexural chord moduli of elasticity. The failure modes were dependent on the orientation of the infill pattern, as the samples printed with the grid pattern in the 0° orientation had a brittle failure mode and the samples with the grid pattern in the 45° orientation had a ductile failure mode. Across most of the samples, the curve of any calculated property followed the same approximate path up until near the point of failure.

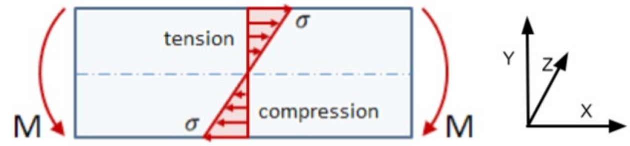

Figure 7. *Diagram of the forces active in a 3-Point Bending test. Adapted from [23]*

IV. Discussion

A. Property Analysis

The primary difference in the samples were their failure modes, and the results strongly suggest that the infill orientation was the cause of it. There is imperfect bonding between the parallel layers in FDM parts that creates a weakness, and the 0° samples had half of their internal filament in layers parallel to the y/z plane provided in **Figure 7**, which depicts the forces active in a 3-Point Bending test. Due to their orientation, the forces were in the same direction as the vulnerability, resulting in the complete failure of the interlayer bonds and a brittle failure mode. On the other hand, in the 45° samples, both layers of filament had their weaknesses offset by 45° to the direction of force and logically the interlayer bonds were more resistant to completely failing. Harpool et al. [13], instead of using flexural tests, conducted tensile tests on FDM samples. They used samples with a 15% infill density and observed that both 0° and 45° samples resulted in ductile failure modes under tensile force. The lack of change in failure modes may have been due to the low infill density resulting in samples that were less stiff and acted similarly to the less stiff 45° samples in the study at hand. However, they did evaluate solid samples with 100% infill density and found that those samples were very stiff and exhibited a brittle failure mode. Based on their results [13], the conclusions made in the study at hand apply primarily to FDM parts that have higher infill densities and that the infill density's influence on the part cannot be ignored.

Since both 0° and 45° samples in the study at hand had no measured differences in their weights and the 45° samples were able to support a maximum load that was 5% higher on average than the 0° samples, it suggests that using a 45° infill orientation results in slightly stronger FDM objects than a 0° infill orientation for the same amount of material used. One explanation for this is that due to the chosen infill pattern consisting of two primary filament directions perpendicular to each other, the 45° samples were able to utilize to some extent filament in both directions to support the load, whereas the 0° samples were unable to use the filament in the direction perpendicular to its length to support almost any part of the load.

Alternatively, despite the 45° samples being able to support heavier loads and having higher flexural strengths, the 0° samples had a 7% higher 0.2% offset yield stress on average compared to the 45° samples. Due to the definition of 0.2% offset yield stress, this means that 0° samples were able to support a 7% higher amount of force before permanently deforming by 0.2%, which indicates that having a 0° infill orientation results in parts that are initially stiffer than parts with a 45° infill orientation. Additionally, the 0° samples had a flexural chord modulus of elasticity that was 13% higher than the 45° samples, which means that 13% heavier loads are required to deform or bend the 0° samples by the same amount as the 45° samples during the linear part of the curve. That suggests that a 0° infill orientation is better in situations where avoiding or minimizing permanent deformation is the priority, but in situations where deformation is acceptable and the ability to withstand a heavier load is prioritized, a 45° infill orientation is better.

The engineering stress vs engineering strain graph in Harpool et al. [13] showed that the samples with a 0° infill orientation were able to support much higher engineering stress values during a tensile test compared to the samples with a 45° infill orientation. This is contrary to the results of the study at hand where both infill orientations resulted in similar flexural stress values. ABS in general tends to have higher flexural strength than tensile strength, which might have caused it to be more sensitive to the tensile forces in [13].

Another study, [19], concluded that when the primary load direction is parallel to the primary filament direction, the mechanical properties are higher. In the study at hand, the 0° samples had 7% higher 0.2% offset yield stress and 13% higher flexural chord moduli of elasticity, which supports the conclusion made in that study. While that conclusion is not always true for the samples evaluated in this study, in the few properties where the 0° samples are weaker, the values for the 45° samples are at most 5% greater than the values for the 0° samples. This is not a negligible difference, but since two of the main flexural properties are much greater in the 0° samples than in the 45° samples, it can be concluded that generally, the conclusion in the earlier study [19] is supported by the results of the study at hand.

Since the 0° samples had coefficients of variation that were much lower than the 45° samples in all calculated flexural properties except flexural strain, where they were only 1% higher, it suggests that fabricating parts with a 3D printer is a much more consistent process when using a 0° infill orientation rather than a 45° infill orientation. One explanation for this is that 3D printers may be more consistent at printing in an isolated x or y direction and less consistent at printing in a diagonal direction. This means that when parts need to be made to specific tolerances and specifications, using a 0° infill orientation is better, but when precision can be sacrificed for additional strength, then a 45° infill orientation is better.

Overall, the data collected in this study suggests that the 0° infill orientation is superior in situations where a stiffer, more precise part resistant to deformation is required, but a 45° infill orientation is superior in situations where the ability to support a larger amount of weight is the highest priority for the part. Additionally, it indicates that using a 0° infill orientation creates risks for a part to snap abruptly and brittlely when it is overloaded but using a 45° infill orientation removes the risk of snapping and results in a ductile failure mode where the part would get weaker as it bends further.

B. Alternative Explanations and Limitations

An alternative explanation for these results is that the differences in the way that the 3D printer prints the 0° infill orientation versus a 45° infill orientation are the cause of the differences in the flexural properties. To elaborate, the printer needs to move horizontally and vertically simultaneously to print a diagonal section as opposed to only needing to move in one direction to print a vertical or horizontal section. That might have caused the 45° parts to have more inaccuracies and weaknesses than the 0° parts, as they are printed primarily with filament running along a diagonal path that is more complicated for a printer to follow. That could mean that the results of this study were only due to the flaws in the printer itself and the effect of infill orientation had little to no impact on a part's flexural properties.

Further research can be utilized to come to a better conclusion about the validity of the alternative explanation. Specifically, another study could investigate whether printing the 45° samples with a 45° angle offset, so that the infill would still be in line with the printer's x and y axes, results in samples that differ greatly from the 45° samples in the study at hand. That would be necessary to determine if the weaknesses in the 45° samples in this study are due to weaknesses in the printer, or if the infill orientation is the primary cause of those weaknesses.

While the conclusions made in this study can be applied to other infill patterns that are structured similarly to the grid infill pattern, little can be concluded about other infill patterns that do not share a similar structure. Additionally, while the 0° and 45° orientations provided the largest variation, it is still necessary to test the angles between those orientations for a more thorough understanding of the anisotropic behaviors. Also, the infill density has been shown to have a large enough influence on the properties of the samples to cause the failure mode to switch from a brittle to a ductile failure mode. Additional studies can investigate how the conclusions made in this study are affected by changes in infill density.

V. Conclusion

The FDM parts with a 0° infill orientation were most resistant to bending and had less variation between replicates of the samples, and the FDM parts with a 45° infill orientation were able to support a higher maximum force. When a bending force was applied, the 0° infill orientation resulted in a brittle failure mode, while the 45° infill orientation resulted in a ductile failure mode. These conclusions are important to the field of study because they provide insight into the extent of influence that the infill orientation has on various flexural properties and thus can be used to make decisions when manufacturing parts with FDM. Furthermore, if these conclusions are not considered when manufacturing an object using FDM, then the object may fail to meet the required standards for its properties, which is extremely dangerous in many industries.

VI. Acknowledgements

Many thanks to Dr. John Gillespie for his knowledgeable guidance and advise throughout the research process. I would like to thank Johnny Thiravong for his instruction regarding the testing of the samples in this study. I would also like to recognize Christopher Meanor for providing access to a 3D printer and his role in building the samples.

References

[1] K. V. Wong and A. Hernandez, “A review of additive manufacturing,” ISRN Mechanical Engineering, 16-Aug-2012. [Online]. Available: https://doi.org/10.5402/2012/208760. [Accessed: 01-Nov-2021].

[2] M. Attaran, “The rise of 3-D printing: The advantages of additive manufacturing over traditional manufacturing,” Business Horizons, 28-Jun-2017. [Online]. Available: https://www.sciencedirect.com/science/article/abs/pii/S0007681317300897. [Accessed: 28-Sep-2021].

[3] M. Habrman, “Influence of the infill on the tensile strength and the economic factors of 3D printing.” [Online]. Available: https://dspace5.zcu.cz/bitstream/11025/36423/1/DAAAM_2019_Habrman.pdf. [Accessed: 01-Oct-2021].

[4] K. Wang, X. Xie, J. Wang, A. Zhao, Y. Peng, and Y. Rao, “Effects of infill characteristics and strain rate on the deformation and failure properties of additively manufactured polyamide-based composite structures,” Results in Physics, 20-Aug-2020. [Online]. Available: https://www.sciencedirect.com/science/article/pii/S2211379720318131. [Accessed: 28-Sep-2021].

[5] J. C. Camargo, A. R. Machado, E. C. Almeida, and E. F. M. S. Silva, “Mechanical properties of pla-graphene filament for FDM 3D printing,” The International Journal of Advanced Manufacturing Technology, 22-Apr-2019. [Online]. Available: https://link.springer.com/article/10.1007/s00170-019-03532-5. [Accessed: 01-Oct-2021].

[6] B. Aloyaydi, “Investigation of infill-patterns on mechanical response of 3D printed poly-lactic-acid,” Polymer Testing. [Online]. Available: https://doi.org/10.1016/j.polymertesting.2020.106557. [Accessed: 01-Oct-2021].

[7] G. Ehrmann and A. Ehrmann, “Investigation of the shape-memory properties of 3D printed PLA structures with different infills,” MDPI, 05-Jan-2021. [Online]. Available: https://doi.org/10.3390/polym13010164. [Accessed: 01-Oct-2021].

[8] A. Elkaseer, S. Schneider, and S. G. Scholz, “Experiment-based process modeling and optimization for high-quality and resource-efficient FFF 3D printing,” MDPI, 22-Apr-2020. [Online]. Available: https://www.mdpi.com/2076-3417/10/8/2899/htm. [Accessed: 27-Sep-2021].

[9] W. M. H. Verbeeten, R. J. Arnold-Bik, and M. Lorenzo-Bañuelos, “Print velocity effects on strain-rate sensitivity of acrylonitrile-butadiene-styrene using material extrusion additive manufacturing,” MDPI, 01-Jan-2021. [Online]. Available: https://www.mdpi.com/2073-4360/13/1/149/htm. [Accessed: 14-Sep-2021].

[10] A. El Moumen, M. Tarfaoui, and K. Lafdi, "Modelling of the temperature and residual stress fields during 3d printing of polymer composites," The International Journal of Advanced Manufacturing Technology, 12-Jun-2019. [Online]. Available: https://link.springer.com/article/10.1007%2Fs00170-019-03965-y. [Accessed: 14-Sep-2021].

[11] A. K. Sood, R. K. Odar, and S. S. Mahapatra, "Experimental investigation and empirical modelling of FDM process for compressive strength improvement," Journal of Advanced Research, 02-Jun-2011. [Online]. Available: https://www.sciencedirect.com/science/article/pii/S209012321100066X. [Accessed: 28-Sep-2021].

[12] H. Gonabadi, A. Yadav, and S. J. Bull, "The effect of processing parameters on the mechanical characteristics of PLA produced by a 3D FFF Printer," The International Journal of Advanced Manufacturing Technology, 02-Oct-2020. [Online]. Available: https://link.springer.com/article/10.1007/s00170-020-06138-4. [Accessed: 28-Sep-2021].

[13] T. D. Harpool, I. M. Alarifi, B. A. Alshammari, A. Aabid, M. Baig, R. A. Malik, A. Mohamed Sayed, R. Asmatulu, and T. M. A. A. EL-Bagory, "Evaluation of the infill design on the tensile response of 3D printed polylactic acid polymer," MDPI, 25-Apr-2021. [Online]. Available: https://doi.org/10.3390/ma14092195. [Accessed: 25-Sep-2021].

[14] O. Basurto-Vázquez, E. P. Sánchez-Rodríguez, G. J. McShane, and D. I. Medina, "Load distribution on PET-g 3D prints of honeycomb cellular structures under compression load," MDPI, 17-Jun-2021. [Online]. Available: https://www.mdpi.com/2073-4360/13/12/1983. [Accessed: 01-Oct-2021].

[15] J. Sárosi, "Investigation of 3D printing parameters affecting the impact strength," ResearchGate, Jul-2021. [Online]. Available: https://www.researchgate.net/publication/353286074_investigation_of_3D_printing_parameters_affecting_the_impact_strength. [Accessed: 14-Sep-2021].

[16] L. Baich, "Impact of infill design on mechanical strength and production cost in material extrusion Based Additive Manufacturing," 01-Jan-1970. [Online]. Available: https://www.semanticscholar.org/paper/Impact-of-Infill-Design-on-Mechanical-Strength-and-Baich/a53d8f604c0a99e907dcccd55503c7c91ec72cf1. [Accessed: 01-Oct-2021].

[17] M. Lalegani Dezaki and M. K. A. Mohd Ariffin, "The effects of combined infill patterns on mechanical properties in FDM process," MDPI, 26-Nov-2020. [Online]. Available: https://doi.org/10.3390/polym12122792. [Accessed: 01-Oct-2021].

[18] C. Lubombo and M. A. Huneault, "Effect of infill patterns on the mechanical performance of lightweight 3D-printed cellular PLA parts," Materials Today Communications, 21-Sep-2018. [Online]. Available: https://www.sciencedirect.com/science/article/abs/pii/S2352492818301600. [Accessed: 07-Nov-2021].

[19] C. Casavola, A. Cazzato, V. Moramarco, and G. Renna, "Mechanical behaviour of ABS-fused filament fabrication compounds under impact tensile loadings," MDPI, 19-Apr-2019. [Online]. Available: https://www.mdpi.com/1996-1944/12/8/1295. [Accessed: 14-Sep-2021].

[20] J. Podroužek, M. Marcon, K. Ninčević, and R. Wan-Wendner, "Bio-inspired 3D infill patterns for additive manufacturing and structural applications," MDPI, 06-Feb-2019. [Online]. Available: https://doi.org/10.3390/ma12030499. [Accessed: 01-Oct-2021].

[21] Standard Test Method for Flexural Properties of Polymer Matrix Composite Materials, D7264/D7264M – 21, 2021.

[22] "Materials engineering," Flexural strength tests of ceramics [SubsTech], 01-Jun-2012. [Online]. Available: https://www.substech.com/dokuwiki/doku.php?id=flexural_strength_tests_of_ceramics. [Accessed: 29-Apr-2022].

[23] "Strength of materials," MechaniCalc. [Online]. Available: https://mechanicalc.com/reference/strength-of-materials. [Accessed: 26-Jun-2022].